

Numerical investigation of non-local electron transport in laser-produced plasmas*

Dong Ya-Lin(董亚林)^{a)b)}, Zhao Bin(赵斌)^{a)b)}, and Zheng Jian(郑坚)^{a)b)†}

^{a)}CAS Key Laboratory of Basic Plasma Physics, University of Science and Technology of China, Hefei 230026, China

^{b)}Department of Modern Physics, University of Science and Technology of China, Hefei 230026, China

(Received 8 April 2007; revised manuscript received 18 April 2007)

Non-local electron transport in laser-produced plasmas under inertial confinement fusion (ICF) conditions is studied based on Fokker-Planck (FP) and hydrodynamic simulations. A comparison between the classical Spitzer-Härm (SH) transport model and non-local transport models has been made. The result shows that among those non-local models the Epperlein and Short (ES) model of heat flux is in reasonable agreement with the FP simulation in overdense region. However, the non-local models are invalid in the hot underdense plasmas. Hydrodynamic simulation is performed with the flux limiting model and the non-local model, separately. The simulation results show that in the underdense region of the laser-produced plasmas the temperature given by the flux limiting model is significantly higher than that given with the non-local model.

Keywords: laser plasma, non-local electron transport, Fokker-Planck simulation, hydrodynamic

PACC: 5265, 5250J, 5225F

1. Introduction

In direct drive laser fusion, it is electron heat flux that transports absorbed laser energy into overdense region of a target, ablates the outer layer of the target, and ultimately compresses the fuel core.^[1,2] Hence, electron transport process plays an essential role in laser fusion. The using of different electron transport models can significantly affect the description of other physical processes.^[3-7] In hydrodynamic simulations, the electron heat flux is usually taken as^[8]

$$q = \min(fn_e v_T T, q_{SH}), \quad (1)$$

where $n_e v_T T$ is the free-streaming flux, f the flux limiter, n_e the electron number density, v_T the electron thermal speed, T the electron temperature, and q_{SH} the classic Spitzer-Härm (SH) heat flux.^[9] However, there are cases that the flux limiting theory is also inadequate. For example, the flux limiting theory cannot predict a preheating phenomenon^[10] and reduced heat flux in a coronal region due to super-Gaussian distributions.^[11-13] It has been acknowledged that the Fokker-Planck (FP) simulation can provide an accurate description of electron heat flux.^[14-18] But the FP simulation is time-consuming, and is difficult to

embed in a hydrodynamic simulation. Instead of the FP simulation, the so-called non-local model of heat flux may provide an effective and computationally efficient alternative in which there is no need to solve the full FP equation. In a non-local model, the electron heat flux is given by

$$q(x) = \int_{-\infty}^{\infty} q_{SH}(x') G(x, x') dx', \quad (2)$$

where $G(x, x')$ is some kernel function. The non-local model can predict the phenomena of flux inhibition and preheating, and has a good agreement with Fokker-Planck simulations. It also provides a numerically more efficient way to implement the simulation in a hydro code. However, the non-local model has its own inadequacies. Primarily, the heat flux is derived only in the case of linear perturbations in a homogeneous plasma, of which the condition is easily broken down in a laser-produced plasma.

In this paper, with the aid of the full FP simulation, we clarify whether the non-local models derived from linear theory can extend to all regimes relating to laser fusion conditions. Not only does this give insight into non-local electron transport, but also it can provide a more accurate non-local model incorporated

*Project supported by the National Natural Science Foundation of China (Grant Nos 10375064, 10575102, 10625523), and the National High Technology Inertial Confinement Fusion Foundation of China.

†Corresponding author. E-mail: jzheng@ustc.edu.cn.

<http://www.iop.org/journals/cp> <http://cp.iphy.ac.cn>

into hydro simulation. We then perform the hydrodynamic simulation with the most suitable non-local transport model, and compare the simulation results with those obtained with the heat flux limiting model.

2. Comparison with Fokker–Planck simulation

In the non-local theory, the electron heat flux depends on the temperature distribution other than the local temperature gradient. On the assumption that there is a small temperature perturbation T_k with a wave number k in a homogeneous plasma, the non-local theory states that perturbed electron heat flux q_k is proportional to the temperature perturbation, i.e.

$$q_k = -ik\kappa T_k, \quad (3)$$

where κ is the generalized thermal conductivity. Generally, coefficient κ is dependent on wave number k . Only in the collisional limit, can κ be independent of the wave vector and reduce to the SH thermal conductivity κ_{SH} . In order to obtain κ in general case, Fokker–Planck simulations must be performed to calculate the ratio of the perturbed heat flux to the temperature perturbation with various values of wave number k . By this way, the generalized thermal conductivity κ_{FP} can be obtained. It has been found that the resulting κ_{FP} can usually be well fitted with the formula

$$\frac{\kappa_{\text{FP}}}{\kappa_{\text{SH}}} = \frac{1}{1 + (\alpha k \lambda_e)^\beta}, \quad (4)$$

where α and β are two fitting factors, and λ_e is the electron mean-free path. Substituting expression (4) into expression (3) and performing an inverse Fourier transform of expression (3) gives the non-local kernel of the heat flux (2),

$$G(\eta) = \int_0^\infty \frac{e^{ik\eta}}{1 + (\alpha k \lambda_e)^\beta} dk, \quad (5)$$

where

$$\eta(x, x') = \frac{1}{\alpha \lambda_e} \int_x^{x'} dx'' \frac{n_e(x'')}{n_e(x')}.$$

The most widely used non-local models are proposed by Luciani, Mora and Virmont (LMV)^[10] and by Epperlein and Short (ES),^[14] separately. Taking $\beta = 2$ in Eq.(5) yields the LMV kernel,

$$G(x, x') = \frac{1}{2\alpha \lambda_e} e^{-\eta}. \quad (6)$$

The ES kernel is obtained by taking $\beta = 1$ in Eq.(5),

$$G(x, x') = \frac{1}{\pi \alpha \lambda_e} \left[\frac{\pi}{2} \sin(\eta) - \sin(\eta) \text{Si}(\eta) - \cos(\eta) \text{Ci}(\eta) \right], \quad (7)$$

where $\text{Si}(x)$ and $\text{Ci}(x)$ are the sine and cosine integrals, respectively.

It should be pointed out that relation (3) is derived in the case that the perturbations are small and their evolutions are linear. However, in the study of inertial confinement fusion (ICF), the laser-produced plasmas are inhomogeneous and their temperatures usually have large gradients which cannot be simply regarded as small perturbations. We need to authenticate the validity of the non-local models by comparing their predictions with those obtained with full FP simulation. Here, the full FP simulation means that no homogeneity and small perturbations are assumed in the FP simulation. For this goal, we develop a FP code based on Epperlein's scheme.^[19] It can describe one-dimensional electron transport in laser-produced plasma in ICF conditions.

In our FP simulation, the ablation of a target by a high-power laser is investigated. An ideal plasma, with ions fixed and an initial electron temperature being 0.1 keV, is irradiated by a laser pulse with a wavelength of 351 nm at a constant intensity of 5×10^{14} W/cm² for over 100 ps. The electron density and temperature profiles at the time of 100 ps are presented in Fig.1

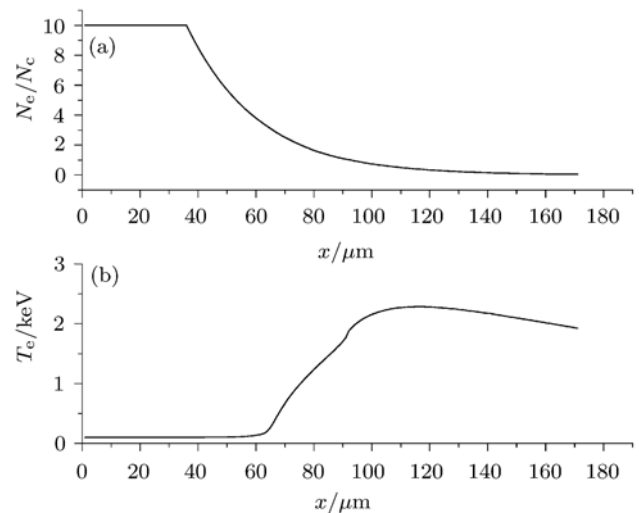


Fig.1. FP simulations of (a) electron number density(normalized to the critical density) and (b) temperature in keV, at the time $t = 100$ ps.

We are interested in the electron heat flux predicted from different models. In Fig.2, we plot the

heat flux given by our FP simulation, the ES model, and the SH theory, separately. As clearly seen from Fig.2, the ES model gives a heat flux in good agreement with our FP simulation in overdense region. This means that the ES model can be an accurate method of describing electron transport in dense plasmas. The heat flux q_{ES} is inhibited in comparison with the classic SH heat flux q_{SH} . In particular, $q_{\text{ES}}/q_{\text{SH}} \approx 0.2$ in the region around the steepest temperature gradient. We zoom in the heat front in Fig.2. It can be seen that the heat flow q_{ES} exceeds the classical heat flow q_{SH} , which is called preheating phenomenon. The preheating phenomenon is a natural consequence of Coulomb collisions whose cross section is inversely proportional to the square of the kinetic energy of charged particles. Energetic electrons that carry the bulk heat flux have a very long mean-free path because of their high energies and cannot be thermalized in a short distance over which the temperature varies significantly. In Fig.3, we plot a typical electron energy distribution where preheating phenomenon happens. As seen in Fig.3, the energy distribution presents a double-Maxwellian structure. The high energy tail is due to the unthermalized energetic electrons that are generated in a hot underdense region and transport into an overdense region with negligible collisions.

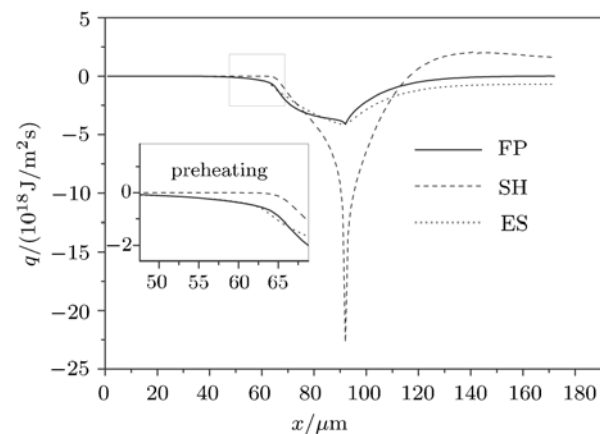


Fig.2. Comparison of the heat flux profiles obtained from Fokker–Planck result, SH result, and ES non-local result at $t = 100$ ps and constant laser intensity $I = 10^{14}$ W/cm².

In the hot underdense region, both the non-local model and the SH theory give different results from the FP simulation. As seen in Fig.4 the SH theory predicts a much larger heat flux than that obtained with the FP simulation. This should be due to the

fact that inverse bremsstrahlung absorption can create a super-Gaussian electron speed distribution,^[12] $f_m(v) = C_m \exp[-(v/v_m)^m]$, where $m = 2$ corresponds to the weak heating limit and $m = 5$ to the strong heating limit. Mora and Yahi^[12] have shown that in the case of small temperature gradients such a speed distribution leads to a strongly reduced thermal conductivity. In Fig.4, we show the electron energy distribution located at the point of $x = 150$ μm . The profile of the electron distribution of our FP simulation lies between $f_{m=2}$ and $f_{m=5}$. It should be pointed out that the experiments performed by Wang *et al*^[7] have also indicated that the electron energy transport significantly deviates from the prediction of the SH theory.

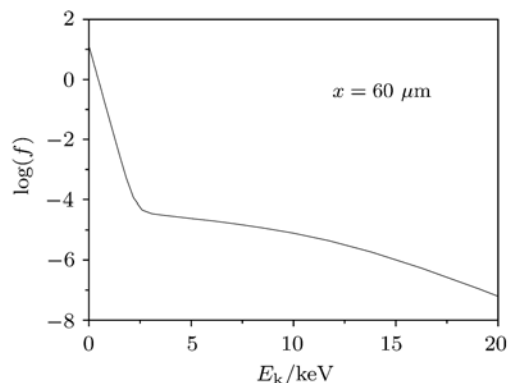


Fig.3. FP simulation of electron distribution $\log(f)$ (in arbitrary units) as a function of electron kinetic energy $E_k = 1/2mv^2$ (in keV) at $x = 60$ μm .

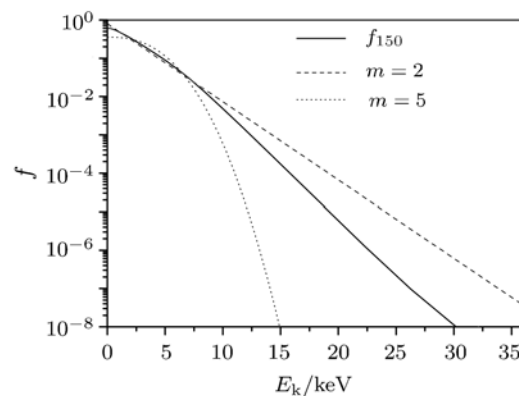


Fig.4. The simulated speed distribution function $f(v)$ at $x = 150$ μm . Function $f_{m=2}$ and $f_{m=5}$ are also plotted for comparison.

The comparison between the results of our FP simulation and the ES non-local model also shows that the ES model becomes invalid in a coronal region. As seen in Fig.3, the heat flux given by the ES model is negative, but that given by the FP simulation is

positive. This is quite understandable. As seen in Fig.3, the classic SH heat flux q_{SH} is very large and negative around a critical region but is small and positive in an underdense region, the convolution given by Eq.(2) can then generate a negative heat flux in the underdense region because the kernel G is delocalized due to the large mean-free path of the electrons in the underdense region.

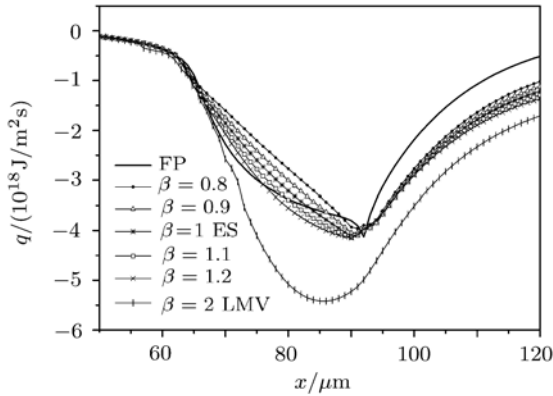


Fig.5. Comparison among heat flux profiles given by different β non-local models using FP simulation.

Several other non-local models have also been proposed. For example, Batishchev and Bychenkov have made a study on the effect of the index β in expression (4) with particle-in-cell and FP simulation in laser-produced plasma with hot spots.^[20–22] In the conditions of interest to them they have proposed $\beta = 0.9$. In Fig.5, we present the heat flux predicted with the non-local model with different values of index β . Within the accuracy of the simulation, we find that when $0.8 < \beta < 1.2$ all non-local models have a reasonable agreement with the FP simulation. But the LMV model gives a prediction far from the FP simulation.

3. Hydro simulation with non-local transport model

Inhibited flux model (1) is most widely used in laser fusion simulations. However, this model has its inadequacies, for example, it fails to predict preheating and overestimates the heat flux in the hot underdense region where the electron distribution tends to be super-Gaussian due to strong inverse bremsstrahlung absorption. Guided by the comparison we made, we incorporate non-local transport model into the hydro simulation. The hydro code with

which we perform the simulation is MULTI1D.^[23] In our simulation, a 0.05 cm thick aluminium disc target at room temperature is irradiated with a train of 351 nm laser pulses under normal incidence. The laser intensity on the target surface is 1.4×10^{14} W/cm². The laser pulse has a Gaussian profile with a full width at half maximum (FWHM) of about 1 ns.

Since the ES model is in good agreement with the FP simulation, we choose the ES model in the hydro simulation. The comparison is made between the flux limiting model and the ES non-local model. It should be pointed out that the non-local heat flux can be parallel to the temperature gradient in the coronal region, which can lead to a numerical instability.^[10] In order to avoid the numerical instability, we enforce the flux q_{ES} to be antiparallel to the temperature gradient.

A comparison between the profiles of the electron temperature obtained with the ES mode and with the flux limiting model is presented in Fig.6. This figure shows the electron temperature distribution at the time of 1.5 ns. As clearly seen in this figure, the temperature given by the flux limiting model is higher than that given by the ES model in the corona region. This result can also be inferred from the discussion given in Section 2. As shown in Fig.2, in the corona region, we have $|q_{SH}| > |q_{ES}| > |q_{EP}|$. So we have $T_{SH} > T_{ES} > T_{FP}$. In the cold matter ahead of the main heat front, the temperature given by the ES model is higher than that given by the flux limiting model because of preheating.

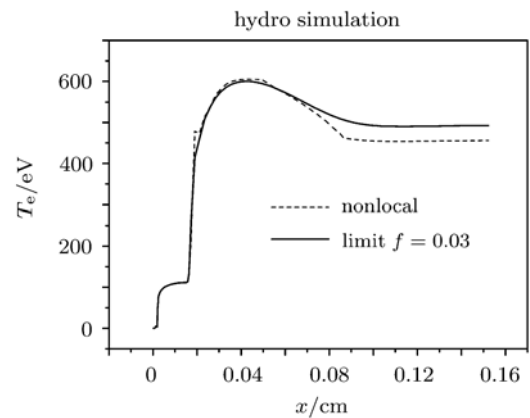


Fig.6. Hydro simulations using non-local model and flux limiting model, of temperature profiles after 1.5 ns irradiation with 351nm laser.

4. Conclusions

We have discussed the non-local electron transport by performing FP simulation and hydrodynamic

simulation. It has been found that the non-local model given by Epperlein and Short is in good agreement with the FP simulation except in a hot underdense region of laser-produced plasmas. We also make a comparison between the flux limiting model and the

ES non-local model by performing hydrodynamic simulation. The simulation results show that in an underdense region the temperature given by the hydrodynamic simulation with the flux limiting model is higher than that given with the ES non-local model.

References

- [1] Lindl J 1995 *Phys. Plasmas* **2** 3933
- [2] Bell A R 1995 *Transport in Laser-Produced Plasmas in Laser Plasma Interactions 5: Inertial Confinement Fusion* (The Scottish Universities Summer School in Physics, Edinburgh) pp139–167
- [3] Ye W H, Zhang W Y and He X T 2000 *Acta Phys. Sin.* **49** 0762 (in Chinese)
- [4] Zheng J, Liu W D and Yu C X 2001 *Acta Phys. Sin.* **50** 721 (in Chinese)
- [5] Gregori G, Glenzer S H, Knight J, Niemann C, Price D, Froula D H, Edwards M J, Town P J, Brantov A, Rozmus W and Bychenkov V Yu 2004 *Phys. Rev. Lett.* **92** 205006
- [6] Wang Z B, Zhao B, Zheng J, Hu G Y, Liu W D, Yu C X, Jiang X H, Li W H, Liu S Y, Ding Y K and Zheng Z J 2005 *Acta Phys. Sin.* **54** 0211 (in Chinese)
- [7] Wang Z B, Zheng J, Zhao B, Yu C X, Jiang X H, Li W H, Liu S Y, Ding Y K and Zheng Z J 2005 *Phys. Plasmas* **12** 082703
- [8] Malone R C, McCorory R L and Morse R L 1975 *Phys. Rev. Lett.* **34** 721
- [9] Spitzer L and Härm R 1953 *Phys. Rev.* **89** 1463
- [10] Luciani J F, Mora P and Virmont J 1983 *Phys. Rev. Lett.* **51** 1664
- [11] Langdon A B 1980 *Phys. Rev. Lett.* **44** 575
- [12] More P and Matte J P 1982 *Phys. Rev. A* **26** 2259
- [13] Zhu S P and Gu P J 1999 *Chin. Phys. Lett.* **7** 520
- [14] Epperlein E M and Short R W 1991 *Phys. Fluids B* **1** 109
- [15] Epperlein E M 1993 *Phys. Plasmas* **4** 3029
- [16] Manheimer W and Colombant D 2004 *Phys. Plasmas* **11** 260
- [17] Colombant D and Busquet M 2005 *Phys. Plasmas* **12** 072702
- [18] Brunner S and Valeo E 2003 *Phys. Plasmas* **9** 929
- [19] Zhao B, Zheng J and Yu C X *Plasma Sci. Technol.* (to be published)
- [20] Bychehkov V Yu and Rozmus W 1995 *Phys. Rev. Lett.* **75** 4405
- [21] Brantov A V, Bychenkov V Yu and Tikhonchuk V T 1998 *Plasma Phys. Rep.* **24** 325
- [22] Batshchev O V, Bychenkov V Yu, Detering F, Rozmus W, Sydora R, Capjack C E and Novikov V N 2002 *Phys. Plasma* **9** 2302
- [23] Ramis R, Schmalz R and Meyer-ter-vehn J 1988 *Comp. Phys. Comm.* **49** 475